

EDX AND X-RAY DIFFRACTION INVESTIGATIONS ON DEPOSITED METAL WITH SAW 2 WIRES TWIN-ARC

Ion MITELEA*, Gheorghe GAVANESCU**

*Politehnica University of Timișoara, Faculty of mechanics. Department of industrial and materials engineering; imitelea@mec.utt.ro

**S.C. Grimex S.A. Tg.-Jiu

Key words: TWIN-ARC welding, EDX, diffraction, heterogeneities

Abstract: In this paper are analyzed chemical heterogeneities formed during solidification of the melted metal, characteristic to SAW TWIN-ARC of low alloyed steels OL52.3k, delivered in plates with 18mm thickness. Variation of Mn and Si is justified both by dendritic grow of the grains and by constitutional sub-cooling.

1. Introduction

Expanding SAW welding for large volumes products is based on high productivity and quality. These two objectives are realized by increasing welding speed and current density.

Experiments revealed that increasing welding speed is limited by the difficult conditions of forming the current, mainly when the operation is conducted by a single electric arc [1, 3].

To increase welding speed without formation of important structural and chemical segregations were developed new technological versions, like [2, 4]:

- SAW with tubular wire;
- SAW with addition of hot wire;
- SAW with increase length of the free end;
- SAW with 2 wire in tandem;
- SAW with 2 wires TWIN-ARC.

The present paper reveals the results of fine structure investigations on square and fillet welded joints from OL52.3k plates 18mm thick. Welding process used was TWIN-ARC with two wires L-61, Ø1,6mm, melted in the same melted pool, with Lincolnweld 780 flux.

The two wires were connected to the same power supply, using a single feeding device and CD reverse polarity current.

From these welded joints were cut metallographic transversal samples investigated with X-Ray diffraction to determine chemical composition heterogeneities of deposited metal and the nature of its structural matrix.

2. Segregation phenomena during melted metal pool crystallization

It is well known that phenomena that intervene during welding process are extremely complex and are characterised by a non-symmetric evolution of metallurgical and thermo-mechanical processes.

Chemical composition of the melted zone varies depending of welding process and welding process parameters. This evolution is both continuous and discontinuous.

The causes of a continuous evolution are:

- physical processes: volatilization of Mn, Ni, Cr, Al, etc.

- chemical reactions between chemical elements, resulting gases inside melted metal (effervescent CO, CH₄, etc.);
- reaction between melted metal and environment (protective gas, slag;
- thermal regime variation;
- fluctuation of the solidification speed;
- dilution – a certain proportion of base material enters in melted pool.

Dilution varies in wide limits depending of welding process; so participation of base material to melted zone formation is total to electron beam welding and reduced to electric arc welding using a covered rod.

The causes for a discontinuous evolution are:

- constitutional sub-cooling, dendritic segregation;
- pollution;
- interruption of gas protection;
- humidity absorbed by pieces, rod cover, wire or inside protective gas;
- in general any internal or external factor that could determine a fluctuation of the parameters that determine a continuous evolution of chemical composition.

The discontinuous evolution of chemical composition of the melted zone leads to a solidification microstructure with a layered aspect more or less periodic.

Non-regularities in dendritic grow of crystalline grains determines lines along the successive positions of liquid-solid interface.

To emphasise quantitative the dendritic segregation energy dispersive X-Ray analysis were made, in many points from the central zone of the weld.

The chemical elements analysed were: Mn, Si, Fe. The electron beam scanned a surface of 60x60µm, determining the three Röntgen lines, specific to the three elements: MnK_α, SiK_α and FeK_α.

In figures 1-4 are presented two dispersion spectrums for each type of welded joint, revealing important variation of concentration of the two main elements presented in the chemical composition.

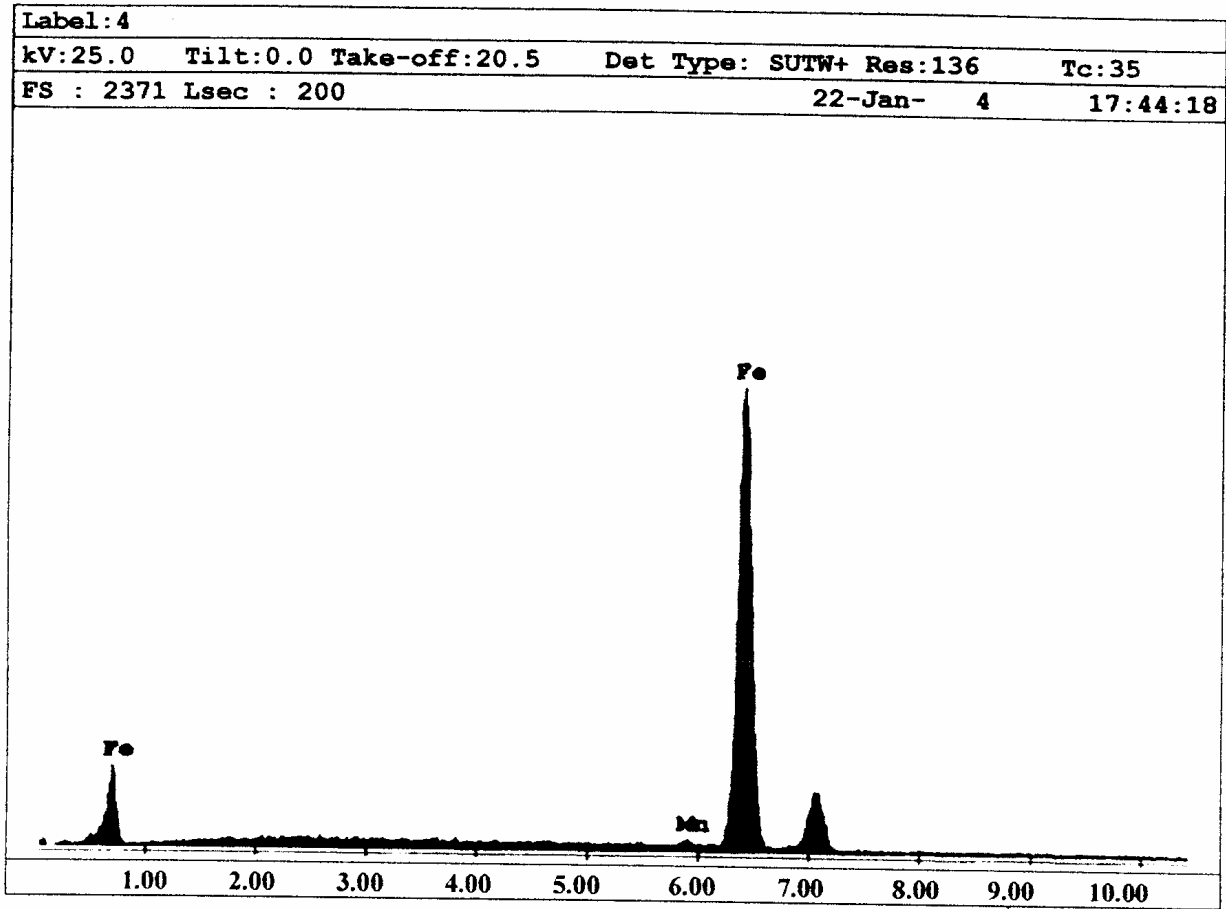
The experimental data demonstrates that Mn concentration varies between 0,71-1,59%mass, in filet weld, respectively between 0,96 and 1,68%mass at square welds. Si concentration varies between 0,66 and 0,86%mass at filet welds and 1,08-1,36%mass at square welds.

These local heterogeneities that accompanies melted pool solidification can be explained by the grain grow process and by constitutional under-cooling phenomena. As we presented before, the grains were growing in a dendritic way, starting from nucleus in well defined directions associated to their crystalline structure (perpendicular on the cube facets).

The directions placed near the direction of solidification trajectory will be privileged for grains grow.

Formation of the first solidification nucleus determines a chemical composition evolution of the neighbouring liquid, delaying its solidification. In this way takes place the constitutional under-cooling phenomena. It is produced step by step and is materialized by creation and grows of the dendrites of variable composition starting with their central part, with higher fusion temperature up to exterior part with lower fusion temperature.

Due to high speed cooling, diffusion homogeneity remains incomplete and chemical heterogeneity maintains after cooling, which determines formation of dendrites and to quantitative variation of chemical elements emphasised by electronic scanning investigations.

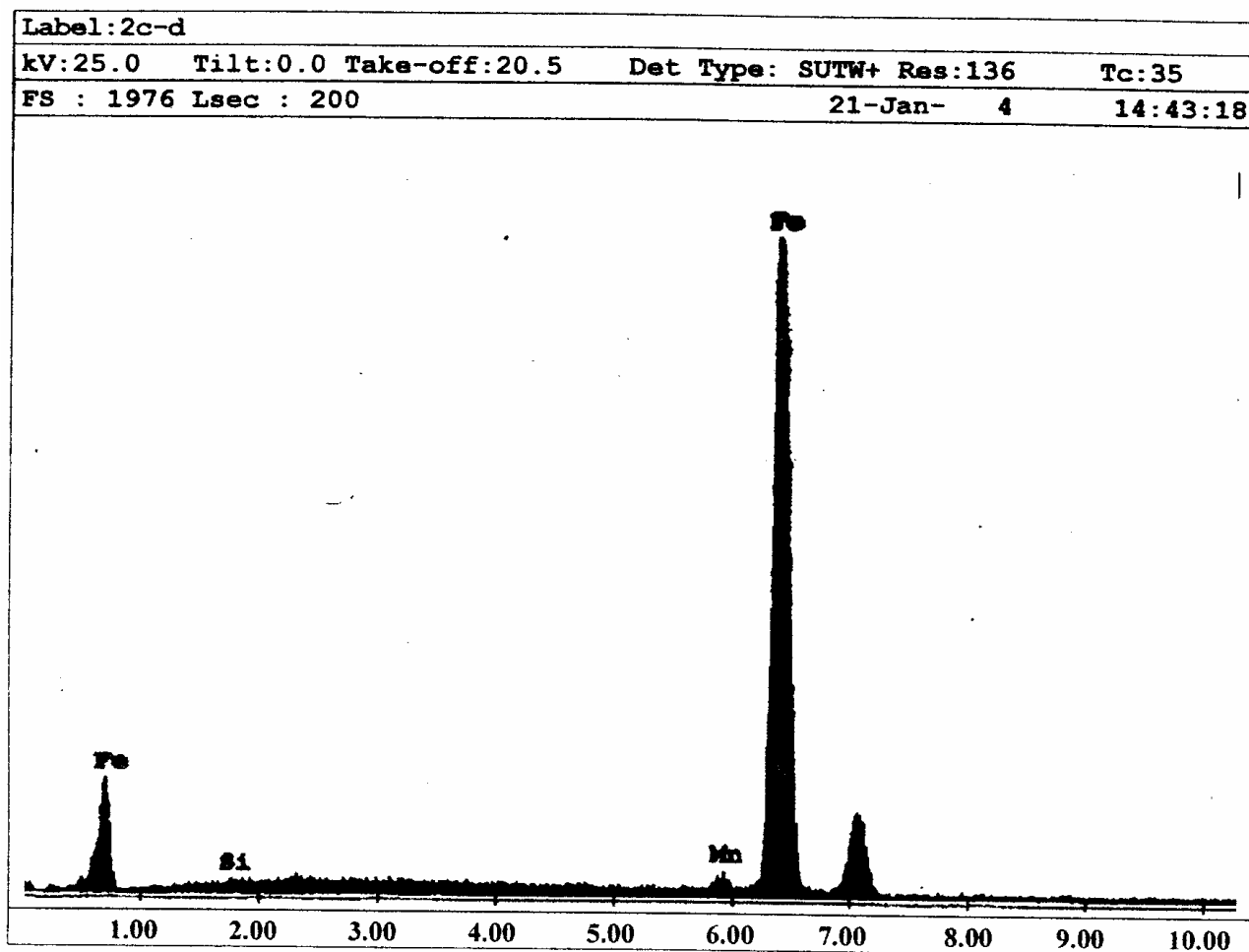


EDAX Quantification (Standardless)
Element Normalized

Element	Wt %	At
MnK	0.71	0.72
FeK	99.29	99.28
Total	100.00	100.00

Element	Net Inte.	Bkgd Inte.	Inte. Error	P/B
MnK	0.69	1.20	14.01	0.58
FeK	88.19	0.96	0.76	92.07

Fig. 1 X-Ray energy spectrum in analysis of central zone of the dendrite crystals inside a fillet welded joint.

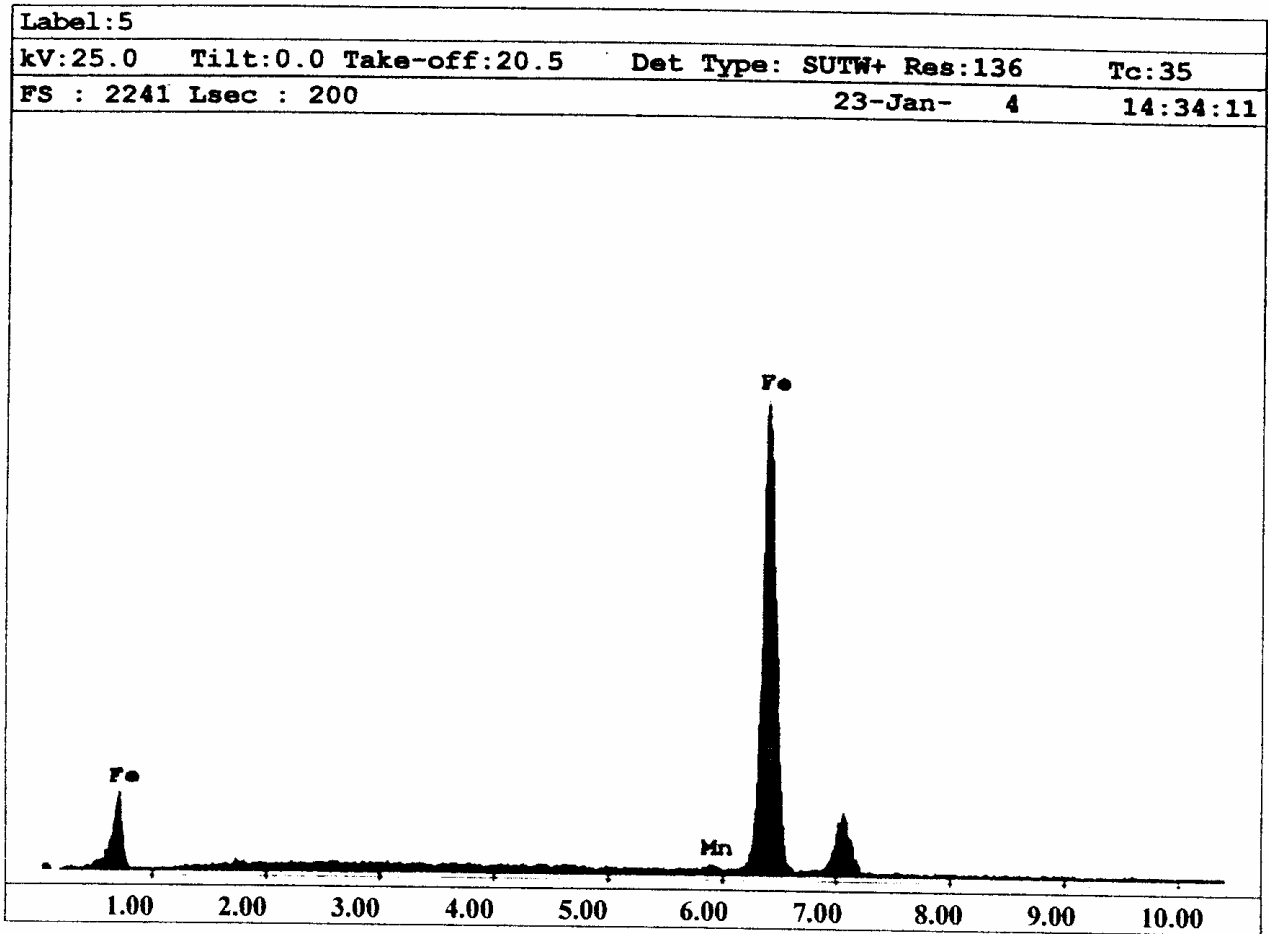


EDAX Quantification (Standardless)
Element Normalized

Element	Wt %	At
SiK	0.66	1.30
MnK	1.59	1.60
FeK	97.75	97.10
Total	100.00	100.00

Element	Net Inte.	Bkgd	Inte. Error	P/B
SiK	0.42	0.88	19.23	0.47
MnK	1.73	1.28	7.08	1.35
FeK	97.33	1.01	0.72	96.07

Fig. 2 X-Ray energy spectrum in analysis of exterior zone of the dendrite crystals inside a fillet welded joint.

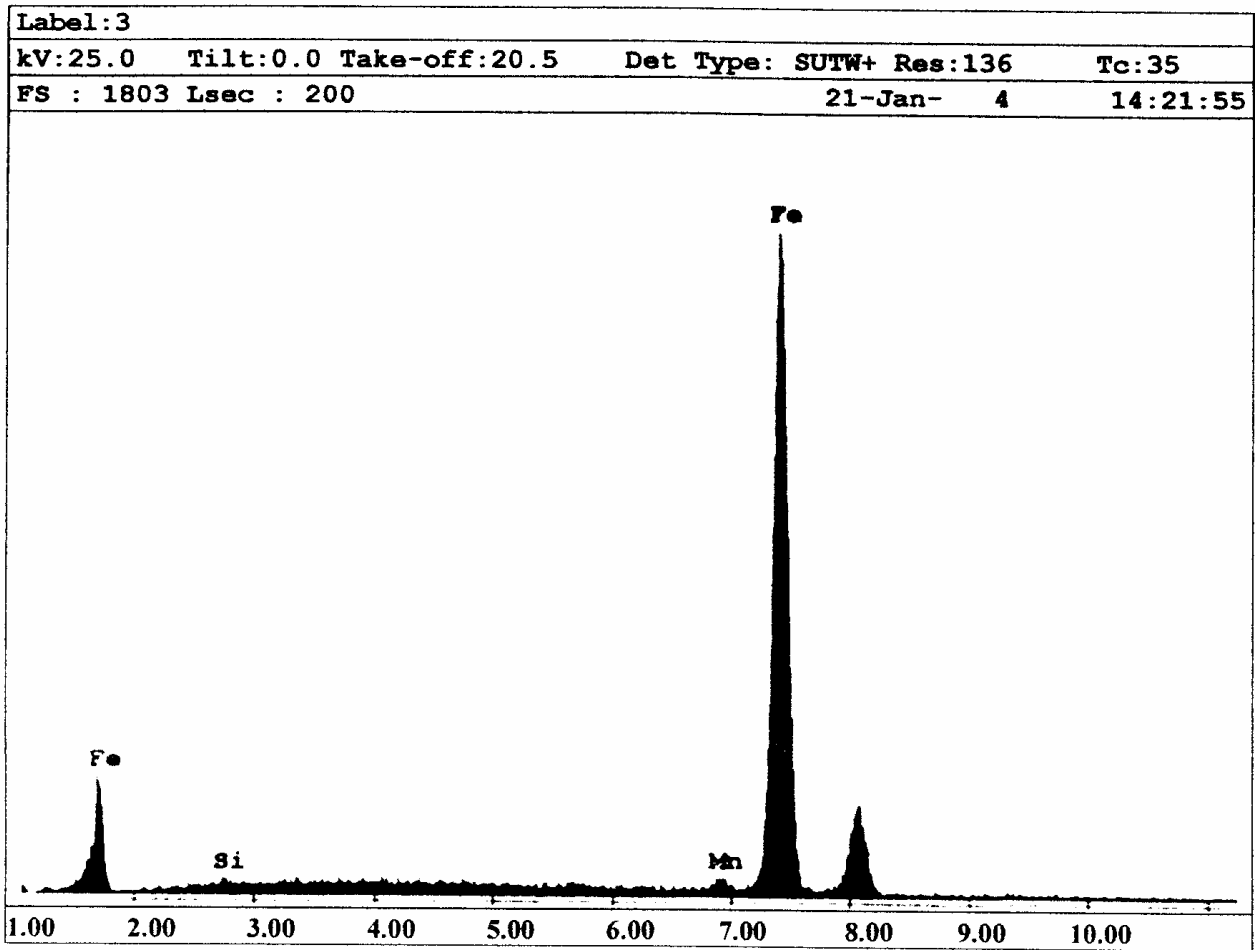


EDAX Quantification (Standardless)
 Element Normalized

Element	Wt %	At
MnK	0.96	0.97
FeK	99.04	99.03
Total	100.00	100.00

Element	Net Inte.	Bkgd	Inte.	P/B
MnK	0.86	0.90	10.86	0.96
FeK	81.66	0.74	0.79	110.50

Fig. 3 Ray energy spectrum in analysis of central zone of the dendrite crystals inside a square welded joint.



EDAX Quantification (Standardless)
Element Normalized

Element	Wt %	At
SiK	1.08	2.12
MnK	1.68	1.69
FeK	97.24	96.19
Total	100.00	100.00

Element	Net Inte.	Bkgd	Inte. Error	P/B
SiK	0.63	0.83	13.48	0.77
MnK	1.69	0.76	6.54	2.22
FeK	89.23	0.60	0.75	148.95

Fig. 4 X-Ray energy spectrum in analysis of exterior zone of the dendrite crystals inside a square welded joint.

3. Phase nature from solidified melted pool microstructure

To identify the base matrix nature from the weld microstructure were carried out X-Ray diffraction analysis.

Scanning parameters used to Röntgen diffractometer Xpert MPD from Philips were:

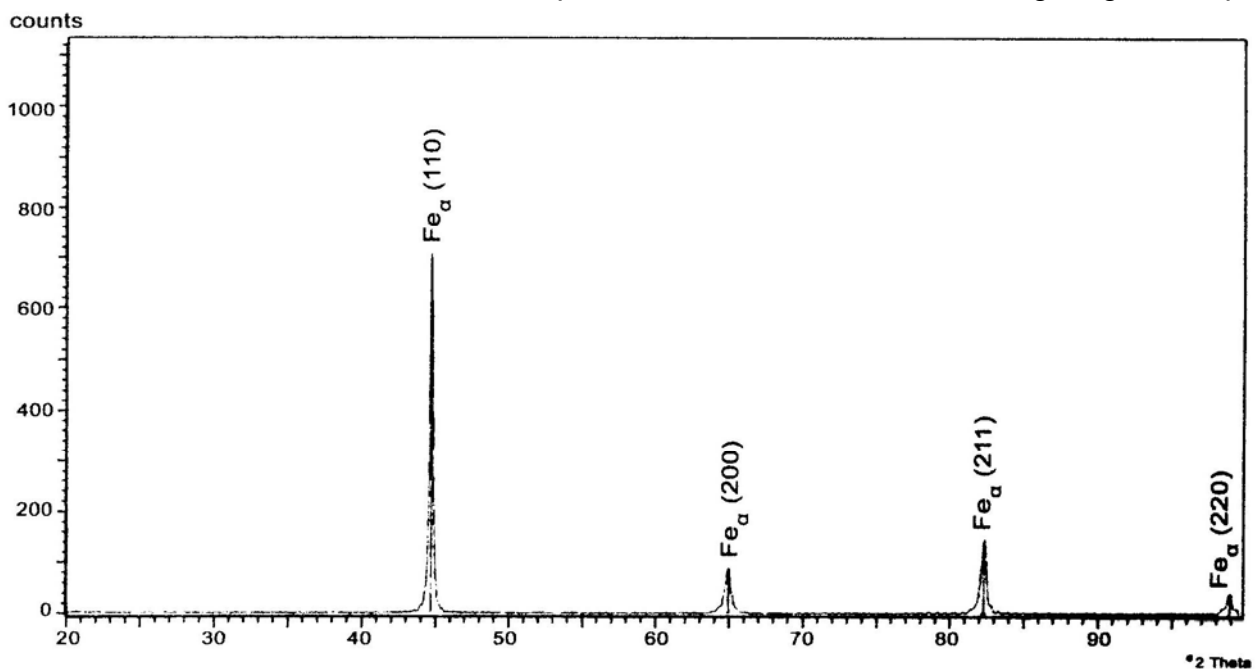
- source: anti-cathode Cu;
- aperture: Soller 1,5°, horizontal 2mm, vertical 8mm;
- filter: Ni 20 μ m;
- time constant: 5s;
- diapason impulse: 10³imp/s;
- room temperature: 25°C.

To record were used the following parameters:

- paper speed: 600mm/h;
- measurement beginning: $2\theta=20^\circ$ and ending $2\theta=100^\circ$;
- counter rotating angle: 1°/min.

In figures 5-7 and tables 1-3 are presented a few records made with X-Ray diffractions. To identify the nature of phases were used existing tables from the data base J. C. POWDER DIFRACTION – ICDD 1996.

Results obtained are corresponding with those obtained in previous investigation, which demonstrates that base matrix structure is ferrite. Obvious that beside ferrite there is a small amount of cementite that was impossible to reveal with this investigating technique.

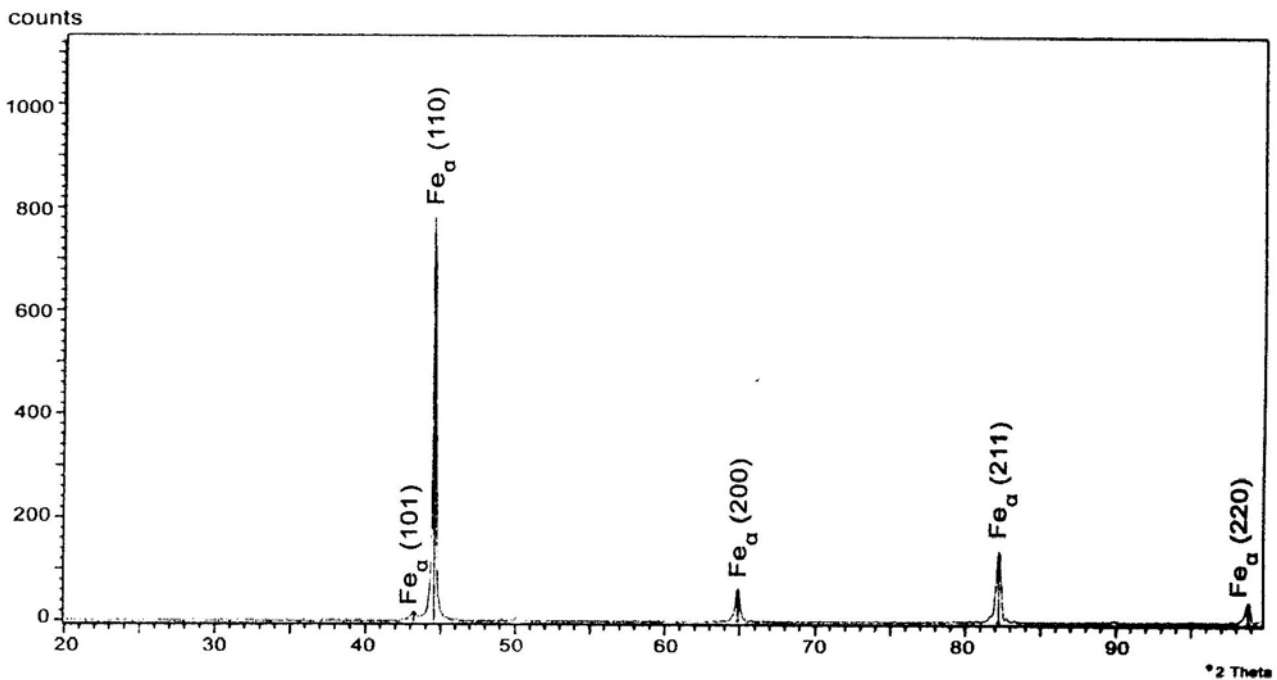


Used wavelength	K- Alpha1
K-Alpha1 wavelength (Å):	1,54056
K-Alpha2 wavelength (Å):	1,54439
K-Alpha2/K-Alpha1 intensity ratio :	0,50000
K-Alpha wavelength (Å):	1,54056
K-Beta wavelength (Å):	1,39222

Fig. 5 Diffraction spectrum characteristic to square welded joint.

Table 1. Distances between crystallographic planes and the high of interference peaks for a square welded joint.

d-spacing (Å)	Relative Intensity (%)	Angle (^o 2Theta)	Peak height (counts)	Beackground (counts)	Tip widht (^o 2Theta)	Significance
2,02638	100,00	44,68300	697,37	3,62	0,20000	5,40
1,43497	12,46	64,93083	86,87	1,72	0,20000	1,05
1,17076	20,40	82,28463	142,23	1,42	0,40000	5,64
1,01378	5,68	98,89552	39,62	0,18	0,25000	1,49

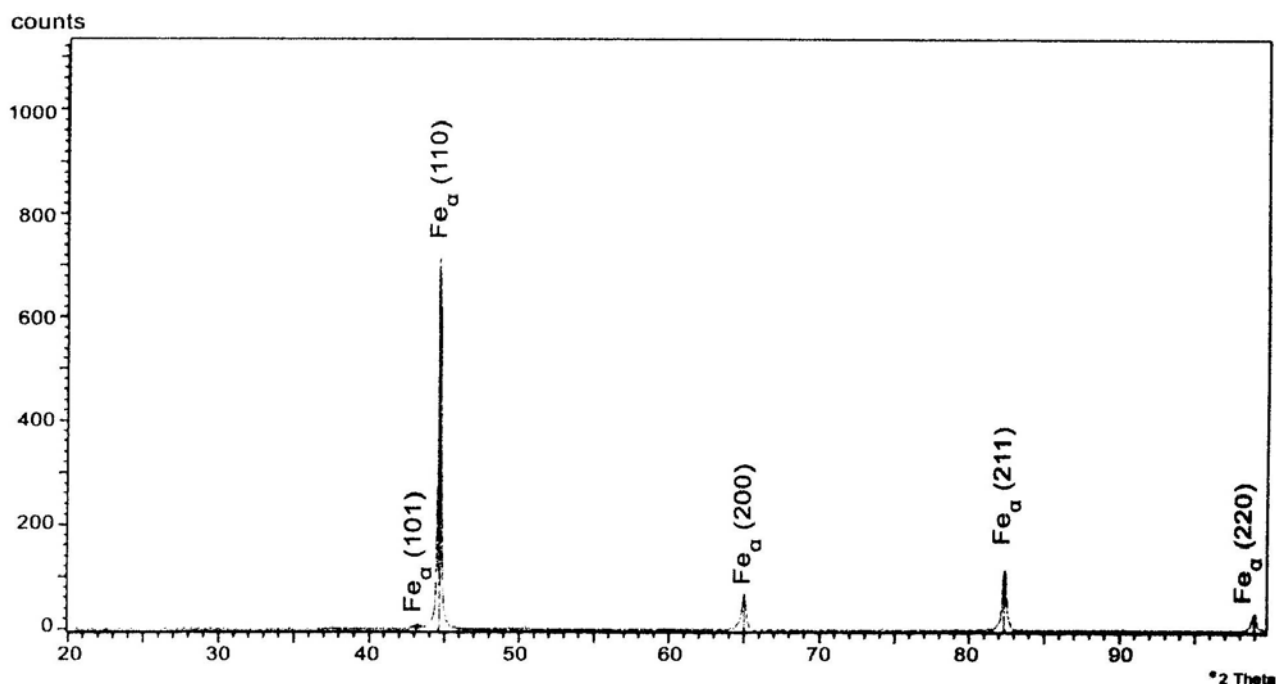


Used wavelength	K- Alpha1
K-Alpha1 wavelength (Å):	1,54056
K-Alpha2 wavelength (Å):	1,54439
K-Alpha2/K-Alpha1 intensity ratio :	0,50000
K-Alpha wavelength (Å):	1,54056
K-Beta wavelength (Å):	1,39222

Fig. 6 Diffraction spectrum characteristic to filet welded joint (first row).

Table 2. Distances between crystallographic planes and the high of interference peaks for a filet welded joint (first row).

d-spacing (Å)	Relative Intensity (%)	Angle (^o 2Theta)	Peak height (counts)	Beackground (counts)	Tip widht (^o 2Theta)	Significance
2,08476	2,32	43,36738	23,03	1,85	0,25000	0,83
2,02498	100,00	44,71545	994,39	1,66	0,20000	8,12
1,43451	8,34	64,95425	82,89	1,04	0,30000	4,01
1,17049	17,81	82,30770	177,08	1,13	0,40000	10,50
1,01364	5,31	98,9133!	52,85	0,75	0,30000	2,90



Used wavelength	K- Alpha1
K-Alpha1 wavelength (Å):	1,54056
K-Alpha2 wavelength (Å):	1,54439
K-Alpha2/K-Alpha1 intensity ratio :	0,50000
K-Alpha wavelength (Å):	1,54056
K-Beta wavelength (Å):	1,39222

Fig. 7 Diffraction spectrum characteristic to file welded joint (second row).

Table 3. Distances between crystallographic planes and the high of interference peaks for a file welded joint (second row).

d-spacing (Å)	Relative Intensity (%)	Angle ($^{\circ}$ 2Theta)	Peak height (counts)	Beackground (counts)	Tip widht ($^{\circ}$ 2Theta)	Significance
2,09000	1,01	43,25313	10,76	2,01	0,50000	0,89
2,02519	100,00	44,71067	1068,98	2,56	0,20000	8,38
1,43445	9,74	64,95744	104,08	1,44	0,25000	2,74
1,17074	16,13	82,2X603	172,43	0,88	0,25000	4,16
1,01380	4,53	98,89191	48,45	1,29	0,25000	1,93

3. Conclusions

Chemical composition heterogeneities that came with melted pool solidification process (Mn concentration variation from 0,71 to 1,59% for fillet welds, respectively from 0,96 to 1,68% for square welds and for Si from 0,66 to 0,86% for fillet welds, respectively from 1,08 to 1,36% for square welds) are justified both by dendritic grow of the grains and by conditional sub-cooling process.

Cooling with relatively high speeds of the melted pool leads to formation and development of dendrites of variable chemical composition, starting with central part which has higher fusion temperature, up to external part, with lower fusion temperature.

X-Ray diffraction demonstrates that for the selected welding parameters, nature of the structural matrix of deposited metal remains ferritic.

BIBLIOGRAHY

1. Hochreiter, G. – Unterpulverschweissen in der Praxis, Expert Verlag Renningen-Malmsheim, 2005.
2. Ishchenko, A. Ya, a. o. – Increase in strength of welds in arc welding of alloy 1420 using the Sc-containing fillers. The Paton Welding Journal, 2002, nr. 1, p. 10-14
3. Müller, P., Wolff, L. – Handbuch des Unterpulverschweissen< Deutscher Verlag für Schweisstechnik GmbH Düsseldorf, 1093
4. Paschold, R., Dirksen, D. – Submerged arc welding of steels for offshore wind towers, Swetsaren, 2005, nr. 1, p. 13-17
5. Pakkari, B. – Tendințe în sudarea și îmbinarea metalelor, Buletinul Institutului Național ISIM Timișoara, 2004, nr. 2, p2-7
6. Pitrun, M., a. o – Correlation of welding parameters and diffusible hydrogen content in rutile flux-cored arc welds, Aus tralasian WELDING, 2004, vol. 49, nr. 1, p. 33-46